Supporting Information

Ru-doped, oxygen-vacancy-containing CeO_2 nanorods toward N_2 electroreduction

Yu Ding, Linsong Huang, Junbo Zhang, Anxiang Guan, Qihao Wang, Linping Qian, Lijuan Zhang, and Gengfeng Zheng**

Laboratory of Advanced Materials, Department of Chemistry and Shanghai Key Laboratory of Molecular Catalysis and Innovative Materials, Fudan University, Shanghai 200438, China.

E-mail: gfzheng@fudan.edu.cn (G.Z.) and zhanglijuan@fudan.edu.cn (L.Z.)

Experimental

Synthesis of CeO_2-Vo. CeO_2 nanorods were synthesized via a hydrothermal method. Briefly, 750 mg of $CeCl_3 \cdot 7H_2O$ was dissolved in 20 mL of deionized (DI) water, and 8.44 g of NaOH was dissolved in 15 mL of water. The NaOH solution was added dropwise into the $CeCl_3$ solution, and this mixture was stirred for another 30 min at room temperature. Then this mixture was placed in a 50-mL Teflon-lined autoclave and heated at 100 °C for 24 h. After cooling, the obtained white precipitate was collected, washed with DI water and ethanol for several times, and then dried in oven at 60 °C overnight. The obtained white precipitate was easily oxidized to CeO_2 in the air. The obtained pale-yellow powder CeO_2 was calcined in a tube furnace under H_2 and Ar mixture atmosphere at 500 °C for 4 h (with a ramping rate: 5 °C /min) to get CeO_2-Vo nanorods.

Synthesis of Ru/CeO_2-Vo and Ru/CeO_2. The CeO_2 and CeO_2-Vo nanorods were then used as precursors to prepare Ru/CeO_2 and Ru/CeO_2-Vo. Specifically, 200 mg of the prepared CeO_2 or CeO_2-Vo nanorods and 15 mg of $RuCl_3 \cdot 3H_2O$ (99% purity, Sinopharm Chemical Reagent Co., Ltd., China) were dispersed in 10 mL of DI water. The pH value was adjusted to 8-9 by Na_2CO_3 solution and stirred for 3 h at room temperature. The Ru/CeO_2-Vo nanorods were washed several times with DI water and ethanol then dried at 60 °C for 12 h.

Electrochemical measurements. All the electrochemical N_2RR tests were conducted with a carbon paper working electrode together with an Ag/AgCl (3.5M KCl) reference electrode in the cathode compartment of a gas-tight H-type cell, separated by the Nafion 117 membrane. A platinum (Pt) counter electrode was placed in the anode compartment. A 0.05 M aqueous H_2SO_4

solution was used as electrolyte. High-purity gas was continuously fed into the cathodic compartment at a constant flow rate during the experiment. All the potentials were calibrated on reversible hydrogen electrode (RHE) according to $E_{RHE} = E + E_R + 0.059 \times pH$ in all measurements in this study. Here, E is the potential measured in all the N_2RR tests; E_R is potential of the Ag/AgCl/3.5 M KCl electrode, which is equal to 0.2046 V; and pH corresponds to the pH in 0.05 M H_2SO_4. The catalyst ink was prepared by uniformly scattering 2 mg of catalysts in 400 μL of ethyl alcohol. Afterwards, 100 μL of the catalyst suspension solution was loaded onto a 1 cm × 0.5 cm carbon paper, followed by drying naturally at room temperature to prepare the working electrode. In order to prevent catalyst falling off during the electrocatalytic process, 5 wt% Nafion ethyl alcohol dispersion was added onto the catalyst side of carbon paper.

Ammonia determination. The concentration of ammonia was qualified by salicylic acid indicator method. Color reagent was prepared by dissolving salicylic acid (5 g), potassium sodium tartrate tetrahydrate (5 g) and sodium hydroxide (8 g) in DI water. Typically, 8 mL of the sample solution was uniformly mixed with 1 mL of color reagent, 0.1 mL sodium nitro-ferricyanide solution, 0.1 mL NaClO solution and DI water to make the total volume as 10 mL and react for 60 min. The formation of indophenol blue was determined using the absorbance at a wavelength of 660 nm by UV-Vis spectrophotometric measurements.

The ammonia product was also detected by ^1H NMR characterization. The electrochemical measurement was conducted by using $^{14}N_2$–saturated 0.05 M H_2SO_4 for different period of time, such as 10 and 20 hours. For comparison, the same electrochemical measurement was carried out in Ar-saturated 0.05 M H_2SO_4 as a control. For NMR measurement, the electrolyte was collected

and concentrated by distillation, and subsequently dissolved in dimethyl sulfoxide-D6. The chemical shifts in the spectra were calibrated using tetramethyl silane (TMS) as an internal standard.

Indicators of ammonia production. Real mass of ammonia production (m) was calculated by the formula as $m = (c_{N2} - c_{Ar} - b) / (k * V)$ (μg). Where $(c_{N2} - c_{Ar})$ is the corrected concentration of produced ammonia calculated by the concentration difference obtained in N_2-saturated and Ar-saturated electrolytes. K and b are the slope and intercept of the standard curve, respectively. V is the volume of the electrolyte solution. Faradaic efficiency (FE) was calculated by $FE = ((3m * F) / 17Q) \times 10^{-6}$, where F is Faraday constant (F = 96,485.34 $C \cdot mol^{-1}$), Q is the total charge passed through the electrochemical system. Ammonia yield rate (YR) was calculated by the formula as $YR = (m / (17t * A)) \times 10^{-3}$ ($mmol \cdot s^{-1} \cdot cm^{-2}$), where t is the reaction time, A is the electrode area of catalysts. Partial current density (P_j) was calculated by $P_j = j * FE \times 10^3$ ($\mu A \cdot cm^{-2}$), where j is the current density of the chronoamperometry curves at different working potentials.

Supplementary Figures and Tables

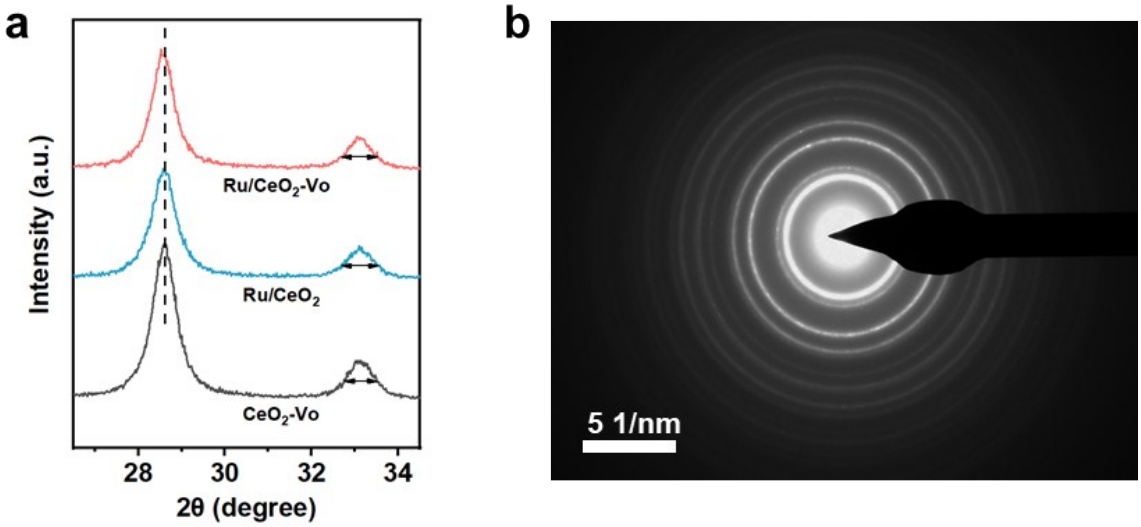

Figure S1. (a) XRD patterns of CeO_2-Vo (black curve), Ru/CeO_2 (blue curve), Ru/CeO_2-Vo (red curve) between 27° and 34°. (b) Selected area electron diffraction (SAED) pattern of Ru/CeO_2-Vo nanorods.

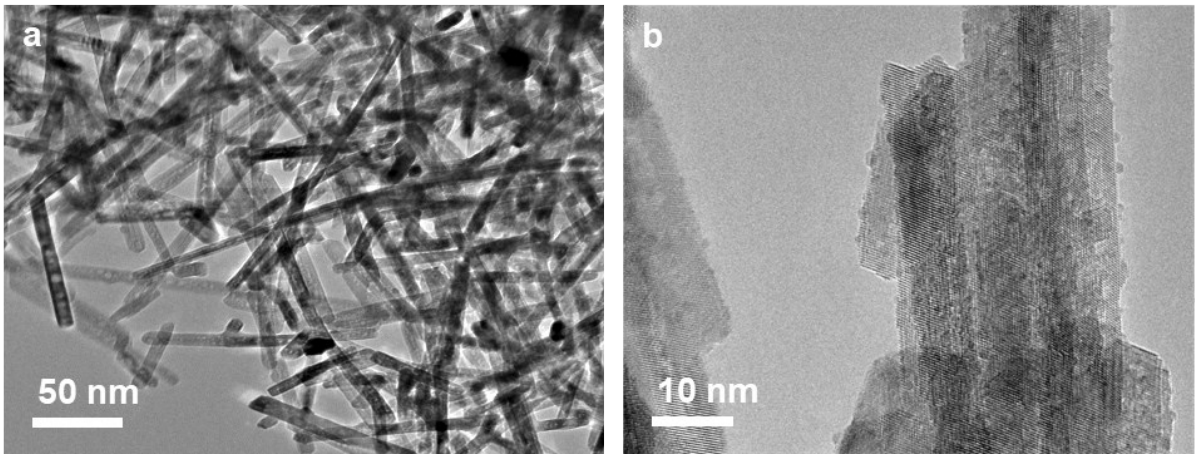

Figure S2. (a) TEM images of CeO_2-Vo nanorods; (b) HRTEM image of Ru/CeO_2 nanorods.

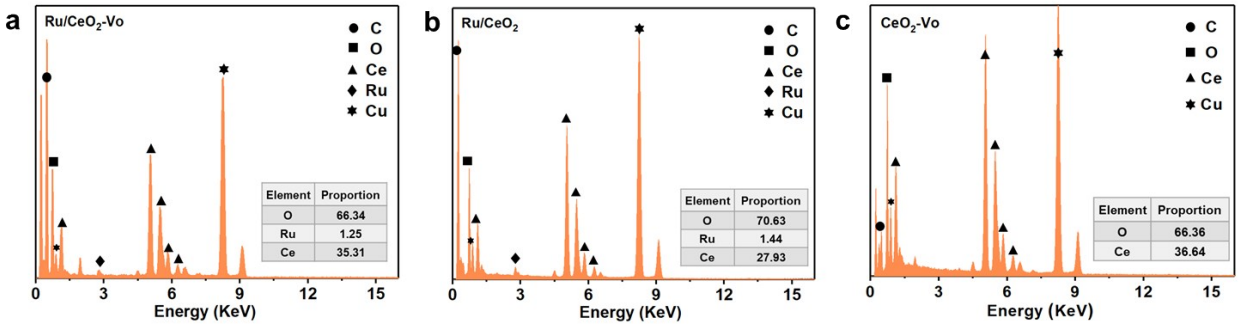

Figure S3. EDS elemental analysis profiles of (a) Ru/CeO_2-Vo, (b) Ru/CeO_2 and (c) CeO_2-Vo nanorods.

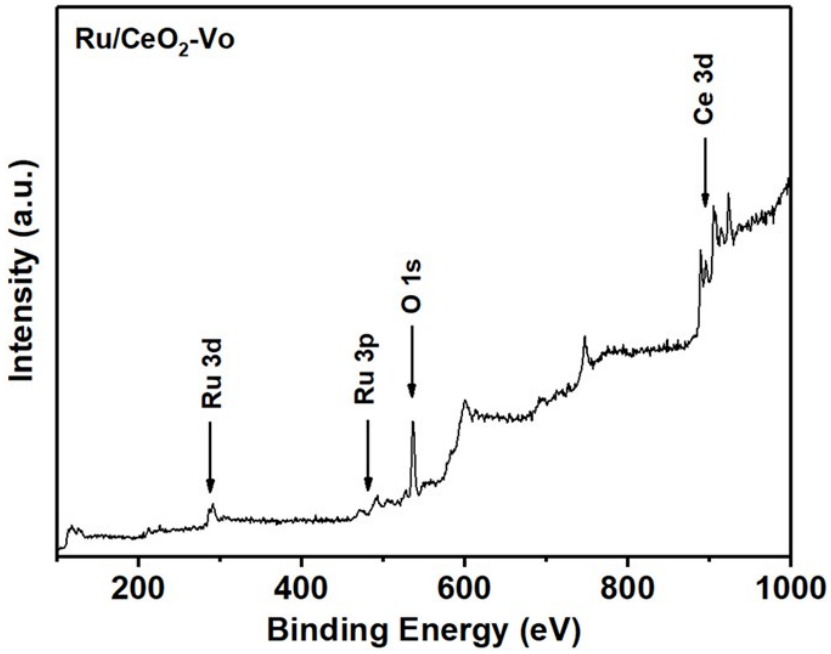

Figure S4. XPS survey spectrum of Ru/CeO_2-Vo.

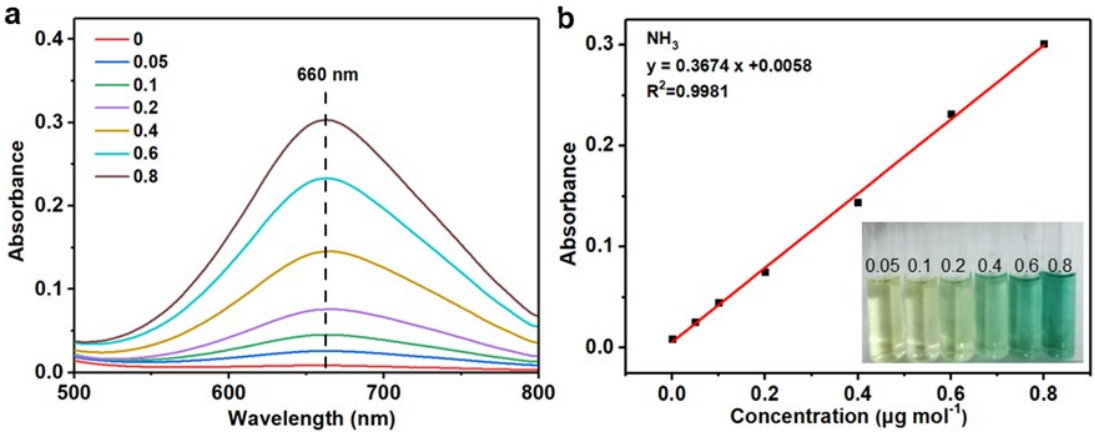

Figure S5. (a) UV-Vis absorption spectra of standard ammonia solutions with salicylic acid indicator. (b) Standard curve for determination of ammonia concentration. Inset shows a picture of colorimetric assays for the standard ammonia solutions after labeling with indicators.

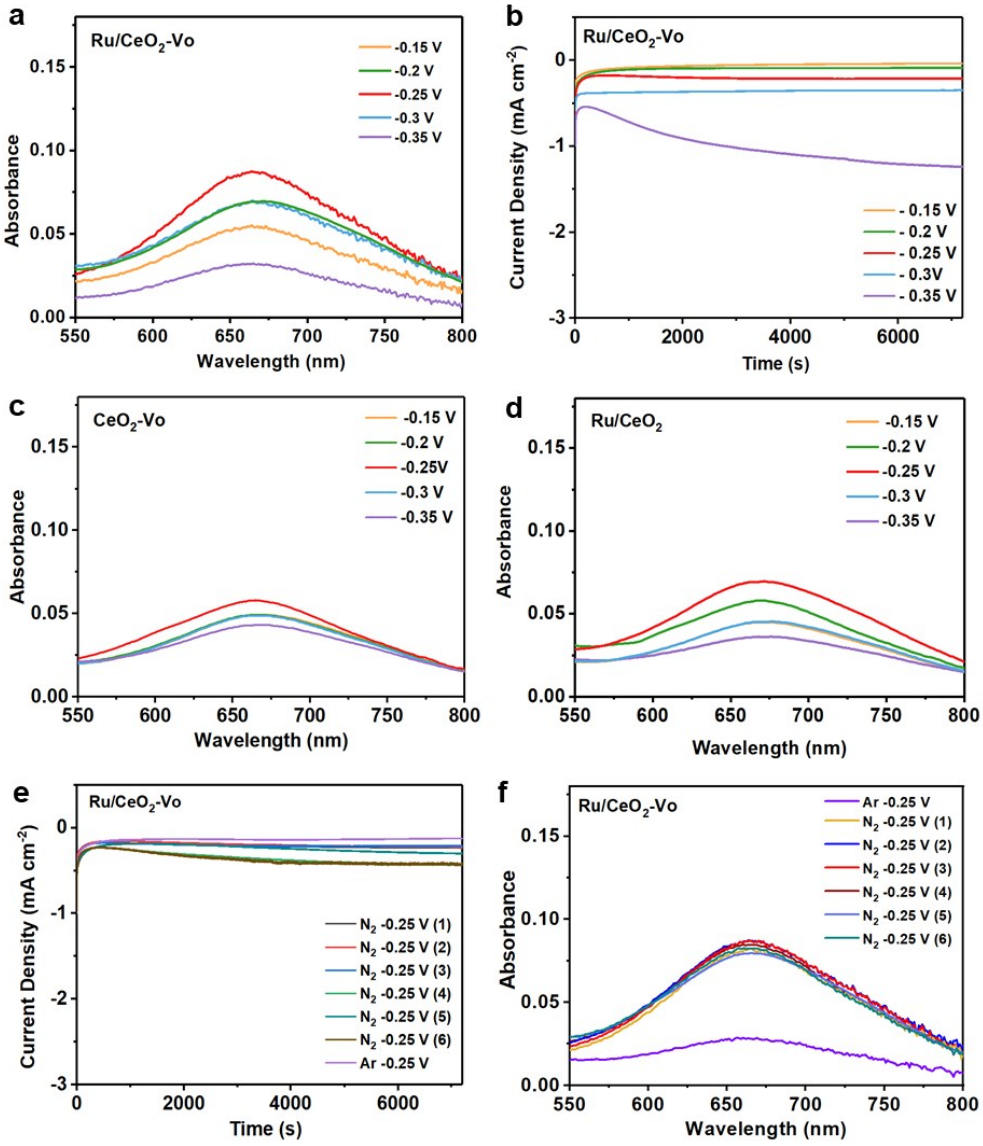

Figure S6. (a) UV-Vis absorption spectra of Ru/CeO_2-Vo. (b) Chronoamperometry curves of N_2RR over Ru/CeO_2-Vo in 0.05 M H_2SO_4 solution at the corresponding potentials. (c, d) UV-Vis absorption spectra of (c) Ru/CeO_2 and (d) CeO_2-Vo after N_2RR electrolysis at different potentials for 2 h. (e) Chronoamperometry curves and (f) UV-Vis absorption spectra of N_2RR over Ru/CeO_2-Vo at the potential of −0.25 V for 6 times. All the yields of ammonia were determined from the standard curve shown ($y = 0.3674x + 0.058$, $R^2 = 0.9981$).

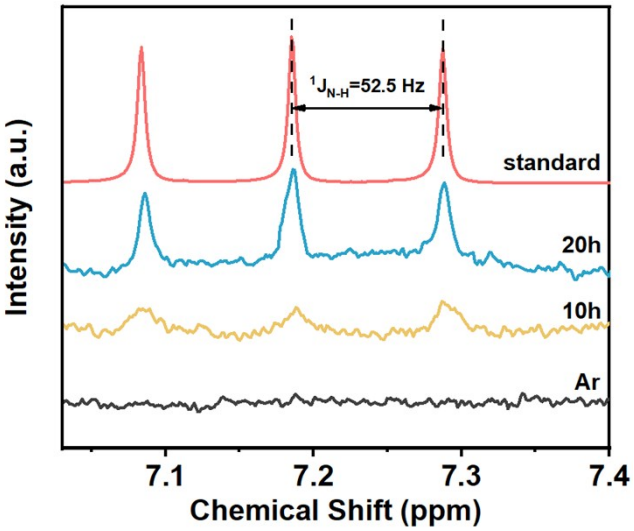

Figure S7. ^{1}H NMR spectra for the $^{14}NH_4^+$ standard sample (red curve), the electrolytes after being electrolyzed with the Ru/CeO_2-Vo nanorods at –0.25 V vs. RHE for 20 h (blue curve) and 10 h (yellow curve) in N_2-saturated 0.05 M H_2SO_4. For comparison, the same Ru/CeO_2-Vo nanorods were also electrolyzed in Ar-saturated 0.05 M H_2SO_4 for 20 h (black curve).

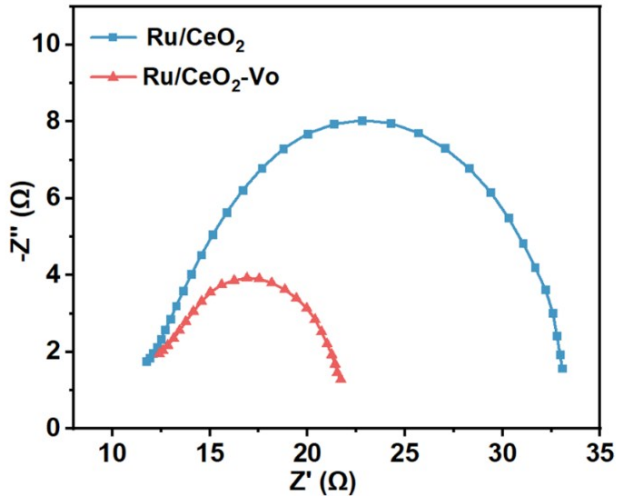

Figure S8. Nyquist plots of Ru/CeO_2-Vo (red curve) and Ru/CeO_2 (blue curve).

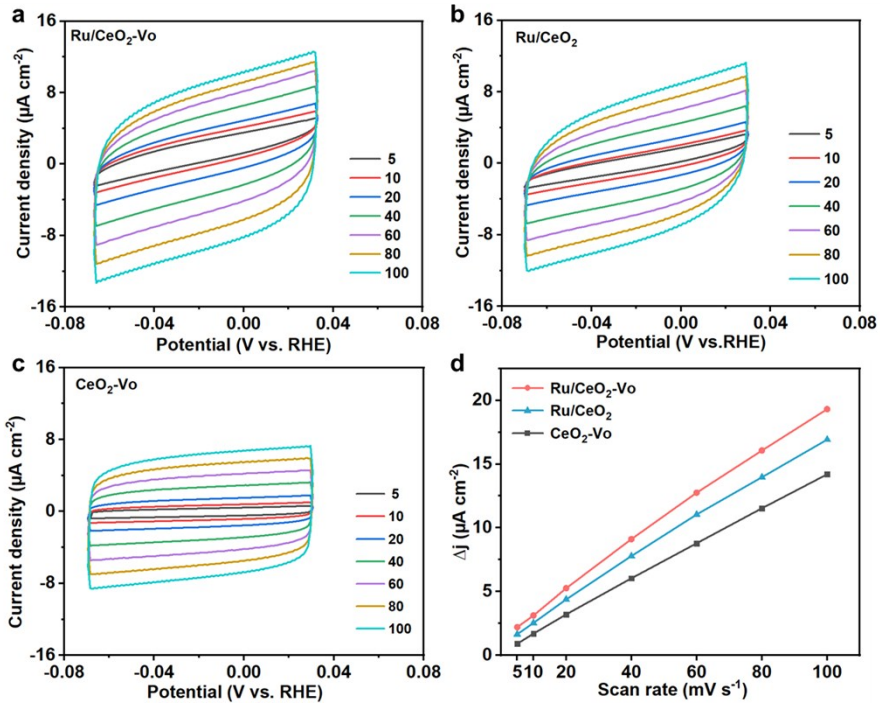

Figure S9. (a) Cyclic voltammetry curves in N_2-saturated electrolyte at different scan rates from 5 to 100 $mV \cdot s^{-1}$ for (a) Ru/CeO_2-Vo, (b) Ru/CeO_2, and (c) CeO_2-Vo. (d) Capacitive current densities vs. scan rate plots of Ru/CeO_2-Vo, Ru/CeO_2 and CeO_2-Vo.

Table S1. SAED analysis of Ru/CeO_2-Vo and the corresponding XRD card.

SAED Test		XRD card				
R	**1/D**	**h**	**k**	**l**	**d**	**Intensity (%)**
3.2	3.125	1	1	1	3.124	100
3.68	2.717391	2	0	0	2.706	27
5.2	1.923077	2	2	0	1.9132	46
6.51	1.536098	3	1	1	1.6316	34
7.11	1.40647	2	2	2	1.5621	6
7.21	1.386963	4	0	0	1.3528	6
7.88	1.269036	3	3	1	1.2414	12
8.21	1.218027	4	2	0	1.21	7
9.02	1.108647	4	2	2	1.1046	10
9.48	1.054852	5	1	1	1.0414	9

Table S2. Relative ratios by different characterizations.

Catalyst	**I_D / I_{F2g}**	**$I_{Ru\text{-}O\text{-}Ce}$ / $I_{summary}$**	**Ce^{3+} / (Ce^{3+}+Ce^{4+})**	**Vo /(Vo+Lo)**
Ru/CeO_2-Vo	14.57%	17.85%	19.19%	56.86%
Ru/CeO_2	5.93%	25.95%	15.44%	46.95%

Table S3. Comparison of the performance of Ru/CeO_2-Vo with other N_2RR catalysts under ambient conditions.

Catalyst	Yield rate	FE (%)	Potential (V vs. RHE)	Reference
Ru/CeO_2-Vo	5.96 μg h^{-1} cm^{-2} (or 9.87 × 10^{-8} mmol·s^{-1}·cm^{-2})	11.7	−0.25	This work
Ru nanoparticles	5.5 μg h^{-1} cm^{-2}	5.4	−0.1	Ref.[S1]
$RuTe_4$	30.4 μg h^{-1} mg^{-1}	0.11	−0.2	Ref. [S2]
Ru SAs/NC	120.9 μg h^{-1} mg^{-1}	29.6	−0.2	Ref. [S3]
Ru dispersed ZIF-8	16.68 μg h^{-1} mg^{-1}	9.2	−0.4	Ref. [S4]
PdRu BPNs	25.92 μg h^{-1} mg^{-1}	1.53	−0.1	Ref. [S5]
FCC PdCu	35.7 μg h^{-1} mg^{-1}	11.5	−0.1	Ref. [S6]
Mo_2C/C	11.3 μg h^{-1} mg^{-1}	7.8	−0.3	Ref. [S7]
CeO_2-D	16.4 μg h^{-1} mg^{-1}	3.7	−0.4	Ref. [S8]
a-Au/CeOx-RGO	8.3 μg h^{-1} mg^{-1}	10.1	−0.2	Ref. [S9]
a-$Bi_4V_2O_{11}/CeO_2$	23.21 μg h^{-1} mg^{-1}	10.16	−0.2	Ref. [S10]

Supplemental References

S1 D. Wang, L. M. Azofra, M. Harb, L. Cavallo, X. Zhang, B. H. R. Suryanto and D. R. MacFarlane, *Chem. Sus. Chem.*, 2018, **11**, 3416–3422.

S2 J. Wang, B. Huang, Y. Ji, M. Sun, T. Wu, R. Yin, X. Zhu, Y. Li, Q. Shao and X. Huang, *Adv. Mater.*, 2020, 1907112, DOI: 1907110.1901002/adma.201907112.

S3 Z. Geng, Y. Liu, X. Kong, P. Li, K. Li, Z. Liu, J. Du, M. Shu, R. Si and J. Zeng, *Adv. Mater.*, 2018, **30**, 1803498.

S4 Z. Zhang, K. Yao, L. Cong, Z. Yu, L. Qu and W. Huang, *Catal. Sci. Technol.*, 2020, DOI: 10.1039/C1039CY02500F.

S5 Z. Wang, C. Li, K. Deng, Y. Xu, H. Xue, X. Li, L. Wang and H. Wang, *ACS Sustainable Chem. Eng.*, 2019, **7**, 2400−2405.

S6 W. Tong, B. Huang, P. Wang, L. Li, Q. Shao and X. Huang, *Angew. Chem. Int. Ed.*, 2020, **59**, 2649–2653.

S7 H. Cheng, L.-X. Ding, G.-F. Chen, L. Zhang, J. Xue and H. Wang, *Adv. Mater.* , 2018, **30**, 1803694.

S8 B. Xu, L. Xia, F. Zhou, R. Zhao, H. Chen, T. Wang, Q. Zhou, Q. Liu, G. Cu, X. Xiong, F. Gong and X. Sun, *ACS Sustainable Chem. Eng.*, 2019, **7**, 2889−2893.

S9 S. J. Li, D. Bao, M. M. Shi, B. R. Wulan, J. M. Yan and Q. Jiang, *Adv. Mater.*, 2017, **29**, 1700001.

S10 C. Lv, C. Yan, G. Chen, Y. Ding, J. Sun, Y. Zhou and G. Yu, *Angew. Chem. Int. Ed.*, 2018, **57**, 6073–6076.